

Effects of bubble size differences on the bubble-trapping performance of arterial line filters

Atsushi Nakamura, Masahiro Kikuta

Abstract

Microbubbles inside a cardiopulmonary bypass circuit are captured by a venous reservoir or by the artificial lung, and ultimately, an arterial line filter (ALF) prevents gaseous micro-emboli (GME) from getting injected into the patient's body. In our study using ALFs with pore sizes of 40 μm (PS40) and 20 μm (PS20), bubbles with a mean bubble diameter of 50 μm , 100 μm , and 180 μm were injected into the ALF. Arterial line filter GME removal was examined using different bubble sizes.

In the bubble group with various bubble sizes, the number of bubbles and the rate of bubble removal were determined for 50 μm bubbles (PS40=44.5 \pm 0.7%, PS20=56.1 \pm 0.6%, $P<0.001$), 100 μm bubbles (PS40=13.7 \pm 1.9%, PS20=9.9 \pm 3.8%, $P=0.205$), and 180 μm bubbles (PS40=-7.0 \pm 1.5%, PS20=-29.3 \pm 1.8%, $P<0.001$). Air bubble shrinkage and bubble volume removal rates were significantly higher with PS20.

The bubble's internal pressure becomes lower as the bubble size is larger, which suggests that air bubbles can easily change shape and disrupt. This suggests that GME removal capability increases when all microbubbles that flow into the ALF are maintained at a diameter of 40-50 μm or less.

Key words : gaseous microemboli (GME), microbubbles, bubble trap performance, arterial line filter

I. Introduction

One reason that cardiopulmonary bypass (CPB) is invasive for the body is the gaseous micro-emboli (GME) in, for example, thin blood vessels such as the capillaries and cerebral and peripheral blood vessels. Microbubbles during a CPB can be caused by drug administration, collection of blood samples, suction in the surgical field, or other events¹⁾. When microbubbles are mixed in the blood, they can cause an embolus in thin blood vessels, with the potential danger of vascular damage or brain dysfunction. Bubbles in the CPB circuit are captured in the venous reservoir, the artificial lung, or elsewhere, and an arterial line filter (ALF) acts as the last line of defense in the CPB

circuit to prevent microbubbles from being transported into the body. However, according to a report on GME removal for CPB circuits, bubbles larger than the ALF pore size have been confirmed at the exit site of the ALF²⁾. An increasing number of GMEs have been found to have been detected after passing through the ALF, and results have shown that many GMEs pass through the ALF³⁻⁶⁾. These research results suggest that the capacity for GME removal is affected by the size of the bubbles flowing into the ALF; however, how different bubble sizes affect the capacity for GME removal remains unclear.

Therefore, in the present study, bubbles of three different sizes were used on ALFs with pore sizes of 40

○Department of Clinical Engineering, Faculty of Health Sciences, Kyorin University

Corresponding Author : Atsushi Nakamura

Department of Clinical Engineering, Faculty of Health Sciences, Kyorin University

5-4-1, Shimorenjaku, Mitaka, Tokyo, 181-8612, Japan

μm ("PS40") and $20\ \mu\text{m}$ ("PS20") to study how different bubble sizes affect the capacity of the ALF in terms of GME removal.

II. Study methods

1. Measurement methods

A hard-shell venous reservoir (CAPIOX-RR-40:Terumo), an artificial lung (CAPIOX-FX25:Terumo), and a centrifugal pump (CAPIOX:Terumo) were used for the experimental circuit design. Multiple pre-bypass filters (PP3802: Pall) with a filter pore size of $0.2\ \mu\text{m}$ were lined up before the bubble generator to prevent bubbles from recirculating in the circuit. The experimental circuit was filled with an aqueous solution of glycerol (2.35 cP, 37°C). The centrifugal pump was set to a flow rate of 4 L/min, and the internal circuit pressure, to 200 mmHg (Fig.1).

The bubbles flowing into each of the ALFs were microbubbles generated by the electrolytic bubble method, in which a perfusion solution is electrolyzed to produce bubbles⁷. Groups of bubbles with a mean bubble size of 50, 100, or $180\ \mu\text{m}$ were generated right before entering the ALFs and were passed into the ALFs. The ALFs of both pore sizes had a fill volume of 100 mL, maximum blood flow rate of 8 L/min, and membrane surface area of $550\ \text{cm}^2$.

Bubbles before and after the ALF were counted with Bubble Counter BC100 (GAMPT). The measurement site was 30 cm from the bubble generation device to the ALFs, with Probe1 (In) placed 10 cm ahead

of the ALFs and Probe2 (Out) placed 10 cm after the ALFs. The bubbles were generated for 20 seconds, from 10 seconds after the measurement was started. Three measurements were taken for each of the settings.

2. Data analysis

The bubble count and volume removal rates (%) were calculated based on the bubble count and volume measured with Probe1 (In) and Probe2 (OUT) of the BC100, respectively. The mean bubble size measured before and after passing through the ALF and the bubble size shrinkage rate (%) from before to after passing through the ALF were determined using the following formulas:

$$\text{Mean bubble size} = \frac{\sum N_i \times D_i}{\sum N_i}$$

N_i = number of bubbles

D_i = respective bubble size

$$\text{Bubble shrinkage rate (\%)} = \frac{(MBS1 - MBS2)}{MBS1} \times 100$$

$MBS1$ = probe1 (Mean Bubble Size)

$MBS2$ = probe2 (Mean Bubble Size)

Statistical processing was performed with SPSS Statistics ver21 (IBM), with the significance set to $P < 0.05$.

III. Results

1. Measurement results

Table 1 shows the bubble count, bubble size, and bubble volume removal rates (%) calculated from the

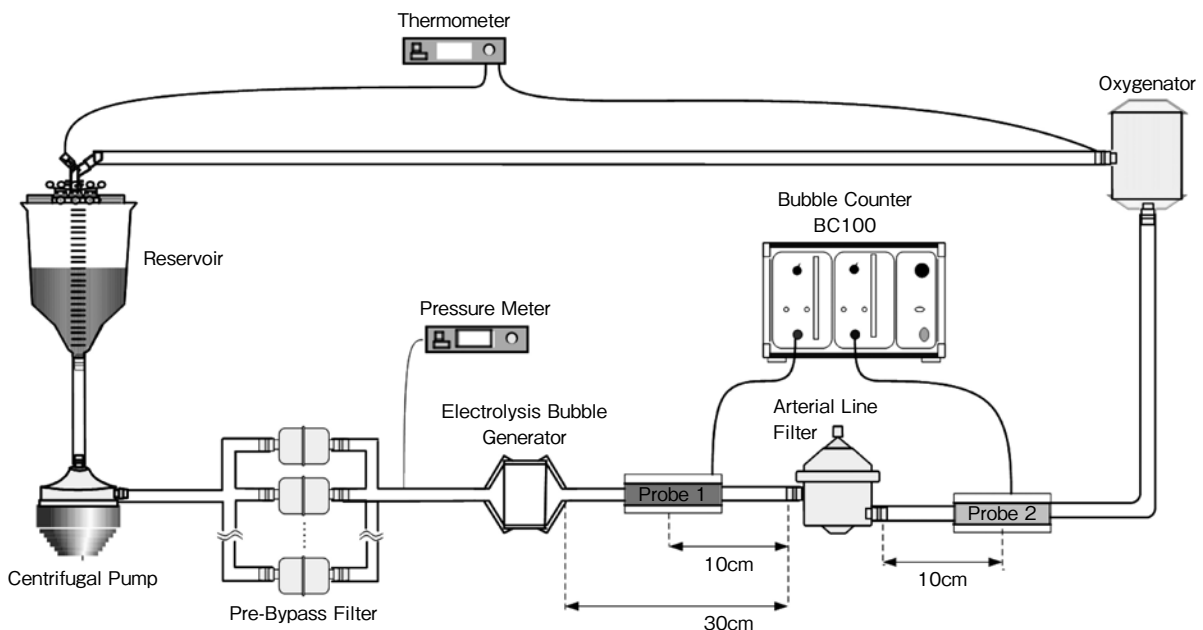


Fig.1 Schematic layout of the experimental circuit

Table 1 Measurement results according to bubbles size

Bubble Size (μm)	Pore Size (μm)	Bubble Count		Mean Bubble Size (μm)		Bubble Volume (nL)		Bubble Count Removal Rate (%)	Bubble Size Shrinkage Rate (%)	Bubble Volume Removal Rate (%)
		In	Out	In	Out	In	Out			
50	40	887.7	492.7	50.9	35.1	172.6	16.0	44.5	30.9	90.6
		(84.2)	(45.1)	(1.5)	(0.6)	(32.6)	(1.9)	(0.7)	(2.4)	(1.3)
		968.3	425.0	51.9	29.3	231.5	7.0	56.1	43.6	97.0
		(42.1)	(20.2)	(0.6)	(0.6)	(17.9)	(0.6)	(0.6)	(0.4)	(0.1)
	P-values	0.212	0.077	0.346	<0.001	0.52	0.002	<0.001	0.001	0.001
100	40	2675.3	2307.7	100.4	51.0	2720.5	239.3	13.7	49.2	91.2
		(185.5)	(113.0)	(2.0)	(0.3)	(190.5)	(19.3)	(1.9)	(1.1)	(0.5)
		2724.0	2454.3	96.8	41.2	2437.0	129.1	9.9	57.5	94.7
		(44.2)	(139.3)	(0.4)	(3.5)	(105.6)	(40.3)	(3.8)	(3.4)	(1.4)
	P-values	0.681	0.23	0.037	0.008	0.087	0.013	0.205	0.016	0.017
180	40	3115.3	3332.7	182.0	87.6	16077.6	1812.8	-7.0	51.9	88.7
		(18.2)	(28.9)	(6.4)	(3.7)	(934.4)	(259.6)	(1.5)	(1.8)	(1.6)
		3296.3	4262.3	181.6	67.7	16578.5	1245.1	-29.3	62.7	92.5
		(7.6)	(49.5)	(0.4)	(0.4)	(235.1)	(15.1)	(1.8)	(0.3)	(0.2)
	P-values	<0.001	<0.001	0.926	0.001	0.419	0.019	<0.001	0.001	0.014

Mean
(Standard deviation)

bubble count and bubble volume measured with Probel (In) and Probe2 (Out) when groups of bubbles with a mean bubble size of 50, 100, and 180 μm were passed into each of the ALFs.

2. Bubble size shrinkage and bubble volume removal rates

The bubble size reduction for PS40 and PS20 in the groups of bubbles according to size were as follows: 50 μm , 30.9 \pm 2.4% and 43.6 \pm 0.4% (P<0.01); 100 μm , 49.2 \pm 1.1% and 57.5 \pm 3.4% (P<0.05); and 180 μm , 51.9 \pm 1.8% and 62.7 \pm 0.3% (P<0.01), respectively, with PS20 having a significantly higher rate of bubble size reduction from before to after the ALF for all bubble sizes. The bubble volume reduction rates were as follows: 50 μm , 90.6 \pm 1.3% and 97.0 \pm 0.1% (P<0.01); 100 μm , 91.2 \pm 0.5% and 94.7 \pm 1.4% (P<0.05); and 180 μm , 88.7 \pm 1.6% and 92.5 \pm 0.2% (P<0.05), respectively, representing a significantly higher rate of bubble volume reduction for PS20 (Figs.2 and 3).

3. Bubble count removal rate

The bubble count removal rate in the group of 50 μm bubbles was 44.5 \pm 0.6% for PS40 and 56.1 \pm 0.4% for PS20, showing a significantly higher bubble count removal rate for PS20 (P<0.001); when the bubble size was 100 μm , it was 13.7 \pm 1.9% for PS40 and 9.9 \pm 3.8% for PS20, indicating no significant difference (P=0.205). When the bubble size was 180 μm , the bubble count removal rate was -7.0 \pm 1.5% for PS40 and

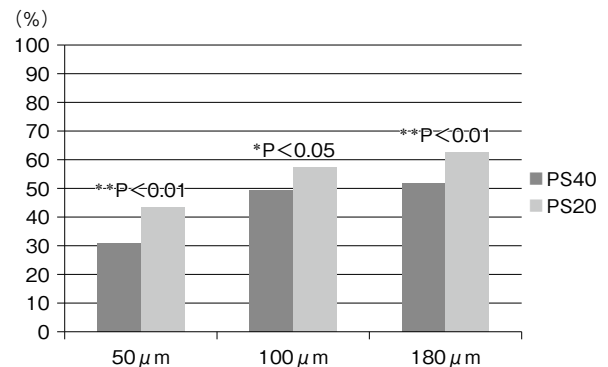


Fig.2 Bubble size shrinkage rate according to bubble size

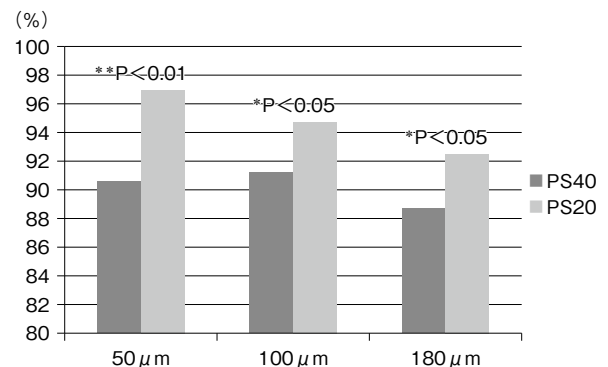


Fig.3 Bubble volume removal rate according to bubble size

-29.3 \pm 1.8% for PS20, with both having an increased bubble count at the exit site as compared with that at the entrance. The results also showed that PS20 had a significantly greater increase than PS40 (P<0.001; Fig.4).

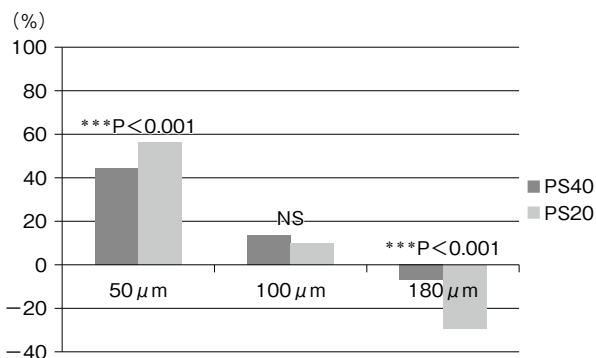


Fig. 4 Bubble count removal rate according to bubble size

IV. Discussion

1. Bubble count removal rate

In their report on GMEs at $\leq 100 \mu\text{m}$, Jabur et al. showed that an ALF with a pore size of $20 \mu\text{m}$ removed admixed emboli at a significantly greater rate than a $40 \mu\text{m}$ filter (33.4% vs 62.1%, $P=0.0029$)⁸. Riley et al., who studied the capacity for bubble removal of 10 different ALFs with pore sizes ranging from 20 to $43 \mu\text{m}$, showed that ALFs with a pore size of $\leq 27 \mu\text{m}$ removed more GMEs⁹. The present study also yielded similar results where the group of $50 \mu\text{m}$ bubbles passed through each of the ALFs ($40 \mu\text{m}$: 44.5% and $20 \mu\text{m}$: 56.1%, $P<0.001$).

The bubble count reduction rate in the group of $100 \mu\text{m}$ bubbles was decreased in contrast to that in the group of $50 \mu\text{m}$ bubbles wherein more bubbles passed through the ALFs. The mean bubble size at the ALF exit side was $51.0 \pm 0.3 \mu\text{m}$ for PS40 and $41.2 \pm 3.5 \mu\text{m}$ for PS20, confirming the presence of bubbles larger than the pore sizes of the ALFs. This suggests that bubbles may have been deformed while passing through the pores of the filters. With the $180\text{-}\mu\text{m}$ bubbles, the fact that both PS40 and PS20 had an increased bubble count at the ALF exit site implies that bubbles may have burst inside and flowed out from the ALF.

2. Bubble deformation and bursting

Normally, when a bubble is stuck onto a filter, it does not pass through the filter if it is larger than the pore size. However, when the pressure outside the bubbles exceeds the pressure inside the bubbles, the bubbles are deformed, causing them to pass through the pores. The pressure at this time is called the bubble point pressure (BPP), which is represented by the following formula (1)¹⁰.

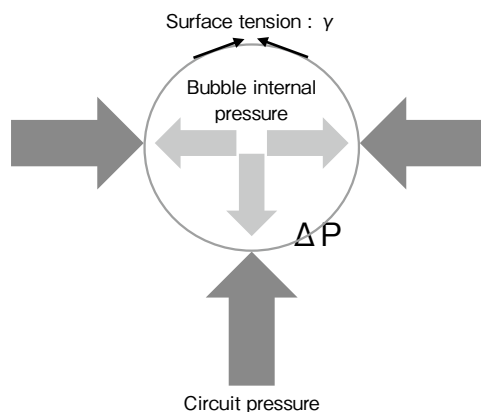


Fig. 5 Relationship between the circuit and bubble internal pressures

$$BPP = \frac{4 \cdot \gamma \cdot \cos \theta}{D} \dots\dots\dots (1)$$

γ : liquid surface tension
 θ : bubble contact angle,
 D : pore size

The relationship between the pressure inside and outside the bubbles is the sum of the internal pressure of the circuit, as per Fig. 5, and the internal pressure of the bubbles according to the Laplace equation, thus yielding the formula (2).

$$\text{Bubble internal pressure (P)} = \text{Circuit pressure} + \frac{4 \times \gamma}{\text{Bubble diameter}} \dots\dots\dots (2)$$

$$\text{Pressure difference } (\Delta P) = \frac{4 \times \gamma}{\text{Bubble diameter}} \dots\dots (3)$$

If the circuit has a constant internal pressure, the internal pressure P of the circuit is inversely proportional to the size of the bubbles, and the pressure inside the bubbles increases. With the bubble size and surface tension, the pressure differential ΔP for inside/outside the bubbles can be calculated using the formula (3).

The pressure differential inside/outside the bubbles that was calculated for each bubble size from the representative values of the surface tension of the solution (Table 2) showed that the larger the bubbles, the smaller the pressure differential inside/outside the bubbles (Table 3). Bubbles with a diameter of $50 \mu\text{m}$ had a pressure of 34.8 to 43.8 mmHg, higher than the internal pressure of the circuit, but this decreased from 21.9 to 17.4 mmHg for $100 \mu\text{m}$ bubbles and from 12.2 to 9.7 mmHg for $180 \mu\text{m}$ bubbles, such that the larger the bubbles, the smaller the pressure difference between inside and outside the bubbles, and the more readily the spherical bubbles deform and pass

Table 2 Surface tension of liquids

	Surface tension (mN/m)
Water (20°C)	73
Glycerin (20°C)	63
Blood (37°C)	58

Table 3 Differences in pressure inside and outside

Bubble diameter (μm)	Water	Glycerin	Blood
50	43.8	37.8	34.8
100	21.9	18.9	17.4
180	12.2	10.5	9.7
250	8.8	7.6	7.0
350	6.3	5.4	5.0

(mmHg)

through the pores. The results of the present study also show the possibility that some 100 μm bubbles were deformed while passing through the pores. Having an outside pressure that exceeded the internal pressure of the bubbles may have caused the 180 μm bubbles to burst, which would explain the increased bubble count on the ALF exit site.

3. Bubble size and volume reduction rates

The results for the bubble size shrinkage and bubble volume removal rates showed that PS20 had greater shrinking effect on the bubbles and reduced the bubble volume. Microbubbles that flow into the ALFs have little buoyancy, and are thus, expected to not flow with the stream, and stick to the filter and remain there. Fiore et al. anticipated that results from simulation using a numerical model for the trajectories of microbubbles would show that a significant number of bubbles with a maximum size of 1,000 μm would be in contact with the filter¹¹⁾. A pore size of 20 μm would theoretically have a two-fold increase from a 40- μm BPP, so PS20 would have a longer time where the bubbles would stick to the filter before passing through the filter, resulting in a higher rate of shrinkage of the bubble diameter and consequently a higher rate of shrinkage of the bubble volume.

4. GME removal efficiency of the CPB circuit

The variation in the results for the GME removal rate of an ALF depending on the size of bubbles flowing are attributed to the fact that the internal pressure of bubbles varies depending on the size of the bubbles. Bubbles of diverse sizes have the potential to flow into the ALF in clinical practice, and if the bubbles flowing into the ALF are large, then results sug-

gest a decreased GME removal efficiency due to the deformation and bursting of the bubbles.

The size of the bubbles flowing into the ALFs affects the venous reservoir filter size. Comparison of filter sizes of 100 to 105 μm and 40 μm for the venous reservoir has yielded results that showed that the GME removal rate was higher with a pore size of 40 μm for the venous reservoir¹²⁾. Groom et al. found that changing the venous reservoir filter size from 105 μm to 30 μm and the ALF pore size from 40 μm to 27 μm reduced the number of microemboli coming from the arterial line of the CPB circuit by 85.7%, from 596 to 80, and reduced the number of microemboli detected in the patient's left and right middle cerebral arteries by 66.1%, from 407 to 138¹³⁾. These reports and the results of the present study suggest that to increase the GME removal rate of a CPB circuit, use of a venous reservoir with a small filter size, keeping all of the bubbles flowing into the ALF between the sizes of 40 to ≤ 50 μm , and use of an ALF with a pore size of 20 μm may be useful to prevent the bubbles from deforming or bursting.

V. Conclusion

According to the present study, the larger the bubbles, the lower the internal pressure inside the bubbles, and thus, the more readily the bubbles deform or burst while passing through the filter. Therefore, although the ALFs have a higher GME removal capacity for bubbles with a size of 50 μm , bubbles with a size of 100 μm deform and pass through the ALF pores. The 180 μm bubbles were also shown to burst, increasing the number of bubbles.

The authors declare that they have no COI.

REFERENCES

- 1) Taylor RL, Feindel CM, et al. : Cerebral microemboli during cardiopulmonary bypass : Increased emboli during perfusionist intervention. *Ann Thorac Surg*, 68 (1) : 89-93, 1999.
- 2) Bakker EWM, Visser K : An in vitro comparison of bubble elimination in Quadrox and Capiox oxygenators. *NESECC UPDATE*, 1 : 20-27, 2011.
- 3) Nielsen PF, Funder JA, Nygaard H, et al. : Influence of venous reservoir level on microbubbles in cardiopulmonary bypass. *Perfusion*, 23 (6) : 347-353, 2008.
- 4) Guan Y, Su X, Undar A, et al. : Evaluation of Quadrox-I adult hollow fiber oxygenator with integrated arterial filter. *The J Extra Corpor Technol*, 42 (2) : 134-136, 2010.

- 5) Melchior RW, Rosenthal T, Glatz AC : An in vitro comparison of the ability of three commonly used pediatric cardiopulmonary bypass circuits to filter gaseous microemboli. *Perfusion*, 25 (4) : 255-63, 2010.
- 6) Qiu F, Peng S, Undar A, et al. : Evaluation of Capiiox FX oxygenator with an integrated arterial filter on trapping gaseous microemboli and pressure drop with open and closed purge line. *Artif Organs*, 34 (11) : 1053-1057, 2010.
- 7) Nakamura A : Basic changes in microbubble characteristics within a cardiopulmonary bypass circuit assessed using bubbles generated by electrolysis. *Jpn J Extra-Corpor Technol*, 41 (4) : 441-450, 2014.
- 8) Jabur GN, Willcox TX, Michell SJ, et al. : Reduced embolic load during clinical cardiopulmonary bypass using a 20 micron arterial filter. *Perfusion*, 29 (3) : 219-225, 2010.
- 9) Riley JB : Arterial line filter ranked for gaseous microemboli separation performance : an in vitro study. *J Extra-Corpor Technol*, 40 (1) : 21-26, 2008.
- 10) De Somer F : Evidence-based used, yet still controversial : arterial filter. *J Extra Corpor Technol*, 44 (1) : 27-30, 2012.
- 11) Fiore GB, Morbiducci U, Redaelli A, et al. : Bubble tracking through computational fluid dynamics in arterial line filters for cardiopulmonary bypass. *ASAIO J*, 55 (5) : 438-444, 2009.
- 12) Myers GL, Voorthees C, Eke B, et al. : Post-arterial filter gaseous microemboli activity of five integral cardiotomy reservoirs during venting : an in vitro study. *J Extra Corpor Technol*, 44 (1) : 20-27, 2009.
- 13) Groom RC, Quinn RD, Likosky DS, et al. : Detection and elimination of microemboli related to cardiopulmonary bypass. *Circ Cardiovasc Qual Outcomes*, 2 (3) : 191-198, 2009.